Interaction of Heparin with a Synthetic Pentadecapeptide from the C-Terminal Heparin-Binding Domain of Fibronectin†

Siva P. Hari, Heather McAllister, Wei-Lien Chuang, Marie Dvorak Christ, and Dallas L. Rabenstein*

Department of Chemistry, University of California, Riverside, California 92521

Received November 19, 1999; Revised Manuscript Received January 18, 2000

ABSTRACT: The synthetic pentadecapeptide FN-C/H II (KNNQKSEPLIGRKKT-NH_2) has the sequence of the carboxy-terminal heparin-binding domain of module III_{14} of fibronectin. Interaction of FN-C/H II with bovine lung heparin has been studied by ^1H and ^{23}Na NMR spectroscopy and by heparin affinity chromatography. FN-C/H II binds to heparin from pD <2 up to pD ∼10; at higher pD, the binding decreases as the lysine side-chain ammonium groups are titrated. Na^+ counterions are displaced from the counterion condensation volume that surrounds sodium heparinate by FN-C/H II, which provides direct evidence that the binding involves electrostatic interactions. The pK_A values for each of the five ammonium groups of FN-C/H II increase upon binding to heparin which, together with chemical shift data, indicates that the binding involves both delocalized and direct electrostatic interactions between ammonium groups of FN-C/H II and carboxylate and/or sulfate groups of heparin. NMR data also provide evidence for the direct interaction of the guanidinium group of the arginine side chain with anionic sites on heparin. The affinity of heparin for FN-C/H II and for 13 analogue peptides in which lysine and arginine residues were systematically substituted with alanine increases as the number of basic residues increases. The relative contribution of each lysine and arginine to the affinity of heparin for FN-C/H II is $R^{12} > K^{13} > K^{14} > K^1 > K^5$. Nuclear Overhauser enhancement (NOE) data indicate that, while FN-C/H II is largely unstructured in aqueous solution, the bound peptide interconverts among overlapping, turn-like conformations over the $L^9 - T^{15}$ segment of the peptide. NOE data for the interaction of FN-C/H II with a heparin-derived hexasaccharide, together with the number of Na^+ ions displaced from heparin by FN-C/H II as determined by ^{23}Na NMR, indicates that the peptide binds to a hexasaccharide segment of heparin. Identical NMR and heparin affinity chromatography results were obtained for the interaction of FN-C/H II and its D-amino acid analogue peptide with heparin, which is of interest for the potential use of peptides as therapeutic agents for diseases in which cell adhesion plays a critical role.

Cell adhesion plays a critical role in the development of many diseases, including arthritis (*1*), metastatic cancer (*2*−*4*), and diseases caused by the invasion of cells by viruses and parasites (*3*). For example, in metastatic cancer, circulating tumor cells attach by cell adhesion to exposed basement membrane of the precapillary venules of the target organ; the attached cells then invade the vascular wall, enter the target organ, and form a secondary tumor colony (*3*, *4*). Cell adhesion is mediated by receptors on the cell surface and ligands of the extracellular matrix or the envelop coat of viruses (*2*−*4*). Receptors include the glycosaminoglycan part of proteoglycans, e.g., the heparan sulfate part of heparan sulfate proteoglycans (*2*, *11*−*13*), and ligands include the cell adhesion proteins fibronectin, laminin, thrombospondin, and vitronectin (*14*−*19*).

Interruption of the cell adhesion process by blocking adhesion sites with synthetic peptides has potential as a therapeutic intervention in the development of diseases in which cell adhesion plays a critical role (*4*, *18*, *20*−*26*). For example, synthetic peptides from the heparin-binding regions of fibronectin and laminin inhibit the experimental metastasis of several metastatic tumor cell types (*2*, *20*, *24*, *25*). The inhibition is correlated with inhibition of adhesion of circulating tumor cells to basement membrane within the pulmonary microcirculation by competitive binding of the peptides to cell surface receptors (*22*). However, knowledge of the interactions involved in the recognition and binding of peptides to cell adhesion sites is limited (*27*−*31*). Such information is of interest for the design of peptides and peptidomimetics with selectivity and high affinity for cell adhesion sites.

With the goal of characterizing in detail at the molecular level the interactions involved in the binding of peptides by the heparan sulfate part of cell surface heparan sulfate proteoglycans, we have initiated studies of the binding of synthetic peptides, using heparin and heparin-derived oligosaccharides as models for cell surface heparan sulfate. Heparin and heparan sulfate are closely related glycosaminoglycans (*14*, *27*, *28*, *32*, *33*). Both are highly negatively charged alternating copolymers of uronic acid (L-iduronic acid or D-glucuronic acid) and D-glucosamine. Their high negative charge density results from the presence of N-sulfamido, ester sulfate and uronic acid carboxylate groups

† This research was supported in part by National Institutes of Health Grant HL56588. Funding for the Varian Unity *Inova* 500 Spectrometer was provided in part by NSF-ARI Grant 9601831.

* To whom correspondence should be addressed. E-mail: dlrab@mail.ucr.edu. Fax: 909-787-2435.

10.1021/bi9926734 CCC: $19.00
Published on Web 03/09/2000

in the disaccharide repeat units. Heparin is largely made up of repeating sequences of the trisulfated disaccharide [→4)-[IdoA(2S)]-(1→4)-[GlcNS(6S)]-(1→], where IdoA(2S)[1] represents 2-O-sulfated iduronic acid (the I ring) and GlcNS(6S)

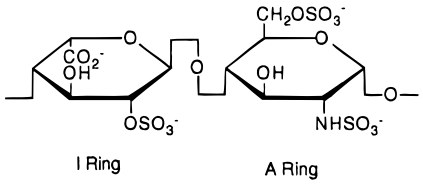

represents N-sulfated and 6-O-sulfated glucosamine (the A ring).

Minor constituents, including the monosaccharides β-D-glucuronic acid (GlcA) and *N*-acetylglucosamine (GlcNAc), and monosaccharides which differ in the location and extent of sulfation, are present in varying amounts, depending on the origin of the heparin (*34*). The structure of heparan sulfate is largely accounted for by the "block-wise" distribution of "heparin-like" segments and segments of the repeating disaccharide [→4)-GlcA-(1→4)-GlcNAc−(1→] (*14*, *35*−*37*). Evidence indicates that the heparin-like segments are involved in heparan sulfate-peptide binding (*35*−*37*), and thus heparin and heparin-derived oligosaccharides with defined patterns of N- and O-sulfation are viable models for heparan sulfate in peptide-heparan sulfate-binding studies (*14*, *27*−*30*, *35*−*38*).

In the first phase of this research, we are studying the binding of synthetic peptides which are known to have a high affinity for heparin, including synthetic peptides based on the heparin-binding regions of cell adhesion proteins. In this paper, we report the results of a study of the interaction of the synthetic pentadecapeptide FN-C/H II (KNNQKSEP-LIGRKKT-NH_2) with heparin. The sequence of FN-C/H II corresponds to residues 1946−1960 in the carboxy-terminal cell and heparin-binding domain of module III_{14} of the cell adhesion protein fibronectin (*21*, *39*). FN-C/H II blocks the adhesion of highly metastatic mouse melanoma cells (*21*, *22*), promotes neural cell adhesion (*39*, *40*), and suppresses arthritis in rats by interrupting leukocyte adhesion and recruitment (*1*). FN-C/H II blocks the adhesion of mouse melanoma cells by binding to the heparan sulfate part of a heparan sulfate proteoglycan receptor for fibronectin on the cell surface (*21*, *22*). The portion which mediates cell adhesion and heparan sulfate binding has been localized to the carboxy-terminal segment LIGRKK (*41*); however, the interactions involved in the binding of FN-C/H II by heparan sulfate have not been characterized. In this work, the interaction of FN-C/H II with heparin has been studied by ^{1}H and ^{23}Na NMR and by heparin affinity chromatography. To elucidate the nature of the binding, the interaction of heparin with analogue peptides in which the basic amino acids and proline were systematically substituted by alanine and with the analogue peptide constructed from D-amino acids (D-FN-C/H II) was also studied.

MATERIALS AND METHODS

Chemicals. FN-C/H II was obtained as a lyophilized powder from Coast Scientific, San Diego, CA, and by synthesis as described below. DCl (35%), NaOD (40%), and D_2O (99.8%) were obtained from Isotec, and sodium 3-(trimethylsilyl)propionate-2,2,3,3-d_4 (TSP) was from Cambridge Isotope Labs. Bovine lung heparin (sodium salt) (146 USP units/mg, 15 000 molecular weight) was obtained from Sigma Chemical Co. The heparin was found to be 80% heparin by comparison of the intensities of the C1−H resonances of the A and I rings of heparin in D_2O solution to the intensities of resonances from imidazole, alanine, and EDTA, which were added as internal intensity standards. The heparin was determined to be 18.2% H_2O from the intensity of the HOD resonance for D_2O solutions of intensity standard without and with heparin present.

Peptide Synthesis. FN-C/H II, 12 analogue peptides in which lysine, arginine, and/or proline were systematically substituted by alanine, and the D-amino acid anaolgues D-FN-C/H II and N-terminal-acetyl-D-FN-C/H II were synthesized using solid-phase peptide synthesis methodology on a Millipore model 9050 Plus peptide synthesizer. Fmoc (9-fluorenylmethoxycarbonyl)-protected amino acids, 1-hydroxy-7-azabenzotriazole (HOAt), 1-hydroxybenzotriazole (HOBt), and 20% piperidine in *N*,*N*-dimethylformamide solution were obtained from Millipore Corp. Fmoc-protected D-amino acids were obtained from Nova Biochem. 5-[4′-Fmoc-aminomethyl-3′,5′-dimethoxyphenoxy] valeric acid-poly(ethylene glycol)-polystyrene (PAL-PEG-PS) resin with a loading capacity of 0.16−0.26 mmol/g was from Millipore Corp, and *N*,*N*′-diisopropyl-carbodiimide (DIPCDI) was obtained from Aldrich Chemical Co.

The Fmoc group was removed from the N-terminal amino group of the resin-bound peptide chain with 20% piperidine in DMF after each amino acid coupling. Incoming amino acids were activated for coupling with HOAt or HOBt and DIPCDI. To maximize coupling efficiency, double coupling was used for amino acids known to be difficult to couple. Unreacted N-terminal amino groups were capped by reaction with acetic anhydride after each coupling cycle. Peptides were cleaved from the resin and side-chain protecting groups removed using a cleavage cocktail which contained 88% trifluoroacetic acid (TFA), 5% phenol, 2% triisopropylsilane, and 5% H_2O (*42*). After cleavage, the solution was filtered through a glass frit of medium porosity, and the filtrate was concentrated on a rotary evaporator. The concentrate was then dissolved in a small volume of TFA, the peptide was precipitated by addition of the TFA/peptide solution to diethyl ether, and the precipitated peptide was purified by reversed-phase HPLC using a Bio-Rad 2800 HPLC system, equipped with either a Bio-Rad Hi-Pore or Vydac reversed-phase C18 semi-prep column. The collected peptide was lyophilized to a white powder. The identify of each peptide was established by fast-atom bombardment mass spectrometry and by NMR, and its purity was determined by HPLC

[1] Abbrebviations: IdoA(2S), 2-*O*-sulfo-α-L-iduronic acid; GlcNS(6S), 2-deoxy-2-sulfamido-6-*O*-sulfo-α-D-glucopyranose; GlcA, D-glucuronic acid; GlcNAc, *N*-acetylglucosamine; ΔUA(2S), 4,5-unsaturated-2-*O*-sulfo-uronic acid; A ring, GlcNS(6S); I ring, IdoA(2S); NMR, nuclear magnetic resonance; T_1, spin−lattice relaxation time; Fmoc, 9-fluorenylmethoxycarbonyl; TFA, trifluoroacetic acid; FN-C/H II, the peptide KNNQKSEPLIGRKKT-NH_2; D-FN-C/H II, the analogue of FN-C/H II constructed from D-amino acids; Hexa1, the heparin-derived hexasaccharide ΔUA(2S)-(1→4)-(GlcNS(6S))-(1→4)-(IdoA-(2S))-(1→4)-(GlcNS(6S))-(1→4)-(IdoA(2S))-(1→4)-(GlcNS(6S); TOCSY, total correlation spectroscopy; NOESY, nuclear Overhauser effect spectroscopy; ROESY, rotating frame Overhauser effect spectroscopy.

and by capillary electrophoresis using a Bio-Rad BioFocus model 3000 instrument. The final peptide products contained trifluoroacetate counterions and residual moisture; the peptide content of each peptide product was determined by ^{1}H NMR.

NMR Measurements. ^{1}H NMR spectra were measured at 500 MHz with Varian VXR-500S or Unity Inova 500 spectrometers. Spectra were measured at 25 °C, unless specified otherwise. Samples were contained in NMR tubes obtained from Norell, Inc. or from Shigemi Co., Ltd. The Shigemi tubes were used to improve elimination of the water resonance by the presaturation method. One-dimensional spectra were measured with the single pulse experiment. Two-dimensional total correlation spectroscopy (TOCSY), nuclear Overhauser effect spectroscopy (NOESY), and rotating frame Overhauser effect spectroscopy (ROESY) spectra were measured with standard pulse sequences (*43*−*47*). Two-dimensional spectra were measured in the phase sensitive mode by the hypercomplex method of States, Habercorn and Ruben (*48*). Typically, spectra were acquired using a spectral width of 5 kHz in both dimensions, 4096 data points were collected in the t_2 dimension, and 256−512 increments were used in the t_1 dimension. NOESY and ROESY spectra were measured using mixing times in the 50−400 ms range; TOCSY spectra were measured using mixing times in the 100−200 ms range. Data were processed with zero-filling to 4096 points in the t_1 dimension, and baseline correction was applied after the first (t_2) Fourier transforms.

^{23}Na NMR spectra were measured at 52.9 MHz and 25 °C with a Varian XL-200 spectrometer. Samples were contained in 5 mm NMR tubes. ^{23}Na spin−lattice (T_1) relaxation times were measured with the inversion−recovery pulse sequence. Relaxation delays of at least $20T_1$ were used in all relaxation time measurements, and spectra were measured at 10−20 different longitudinal relaxation periods in the inversion−recovery pulse sequence. T_1 values were obtained from a three-parameter (I_o, A, and T_1) fit of the inversion−recovery data to the equation $I_t = I_o(1 - A\, e^{-t/T_1})$.

Sample Preparation. ^{1}H NMR measurements were made on D_2O or 90% H_2O−10% D_2O solutions. A small amount of TSP was added for a chemical shift reference. The pH was measured directly in the NMR tube using an Ingold combination ultramicroelectrode. pD values reported for D_2O solutions were corrected for the deuterium isotope effect with the equation $pD = pH_{meter\ reading} + 0.40$ (*49*).

Solutions were prepared for the ^{23}Na NMR studies by dissolving weighed amounts of heparin, FN-C/H II, and NaCl in D_2O. The initial pD of the solution was adjusted to 12, and the ^{23}Na T_1 was determined. The pD of the solution was then lowered in increments of 0.5−1 pD unit by addition of DCl to the NMR tube, and the ^{23}Na T_1 was remeasured. This procedure was repeated until a pD of ∼2 was reached. With this procedure, the Na^+ concentration remained constant as the pD of the solution was changed.

Heparin affinity chromatography experiments were performed on a Dionex 500 HPLC system equipped with a Bioscale MT5 column (10 × 64 mm) packed with Affi-gel heparin affinity chromatography support. Peptides were dissolved in low-salt buffer (5 mM sodium phosphate, pH 5.5) to a concentration of 1 mM, and 20 μL of peptide solution was injected onto the column. Peptides were eluted off the column using a linear gradient of low-salt buffer (solvent A) and 5 mM sodium phosphate, 2 M NaCl, pH 5.5 (solvent B). After injection of the sample, solvent A was passed through the column for 10 min at a flow rate of 2 mL/min. The NaCl concentration was then increased at a rate of 33 mM/min with solvent B until the peptide was eluted. The Na^+ concentration at which peptides were eluted from the column (the Na^+ concentration at peak maximum) was calculated using the elution time and the composition of the two solvents and was also determined directly by conductivity measurements. The conductivity measurements were made on fractions collected at 1 min intervals with a Bio-Rad model 2128 fraction collector.

Hexasaccharide Preparation. The heparin-derived hexasaccharide ΔUA(2S)-(1→4)-[GlcNS(6S)]-(1→4)-[IdoA(2S)]-(1→4)-[GlcNS(6S)]-(1→4)-[IdoA(2S)]-(1→4)-[GlcNS(6S)] (Hexa1) was prepared by depolymerization of bovine lung heparin with heparinase I (Sigma Chemical Co.) (*50*). One gram of heparin dissolved in 50 mL of solution containing 0.1 M sodium acetate (pH 7.0), and 10 mM calcium acetate was combined with 250 units of heparinase I. After depolymerization, the reaction solution was concentrated by lyophilization, and then 0.2 g portions of the mixture of oligosaccharides were size fractionated by gel permeation chromatography using a 3 cm × 200 cm column packed with Bio-Rad Bio-Gel P6 resin and a 0.5 M $(NH_4)HCO_3$ eluent. The separation was monitored by measuring the absorbance at 232 nm. The hexasaccharide fraction was desalted by lyophilization and then further separated according to charge by strong anion-exchange (SAX) chromatography using the Bio-Rad 2800 HPLC system equipped with a 10 mm × 250 mm Spherisorb (5 μm) SAX column (Thomson Inst. Co.) and a linear gradient of 0.2 M NaCl (solvent A) to 1.4 M NaCl (solvent B) at pH 3.5 at a flow rate of 1.5 mL/min (0−10% B in 10 min, then 10−100% B in 135 min). Each HPLC fraction was desalted on a Sephadex G-10 column (3 × 70 cm). The fraction corresponding to Hexa1 was identified by ^{1}H NMR, using chemical shifts obtained for each of the carbon-bonded protons on each of the six residues from 2D-TOCSY spectra. The resonances were assigned to specific IdoA(2S) and GlcNS(6S) monosaccharides of Hexa1 using interresidue NOEs obtained from ROESY spectra. Assignment of the structure was confirmed by comparison of the chemical shifts and coupling constants to literature values (*51*−*53*).

RESULTS

^{1}H NMR Studies of FN-CH II−Heparin Binding. The heparin used in this research has an average molecular mass of 15 kDa, which corresponds to ∼25 disaccharide repeat units. To determine a suitable stoichiometry at which to study the binding of FN-C/H II by heparin, ^{1}H NMR spectra were measured for a 5 mM solution of FN-C/H II plus heparin at heparin disaccharide repeat unit-to-peptide ratios ranging from 0:1 to 5.2:1 at pH 5.5. As the ratio was increased, the ^{1}H NMR spectrum of the peptide changed, most notably in the amide NH region, and then remained constant at ratios ≥4:1. A ratio of ≥4:1 and a pH of 5.5 were used in most of the ^{1}H NMR studies.

^{1}H NMR spectra of FN-C/H II, heparin, and FN-C/H II plus heparin were assigned by standard methods (*54*, *55*). Resonances for the peptide backbone amide protons (7.8−9

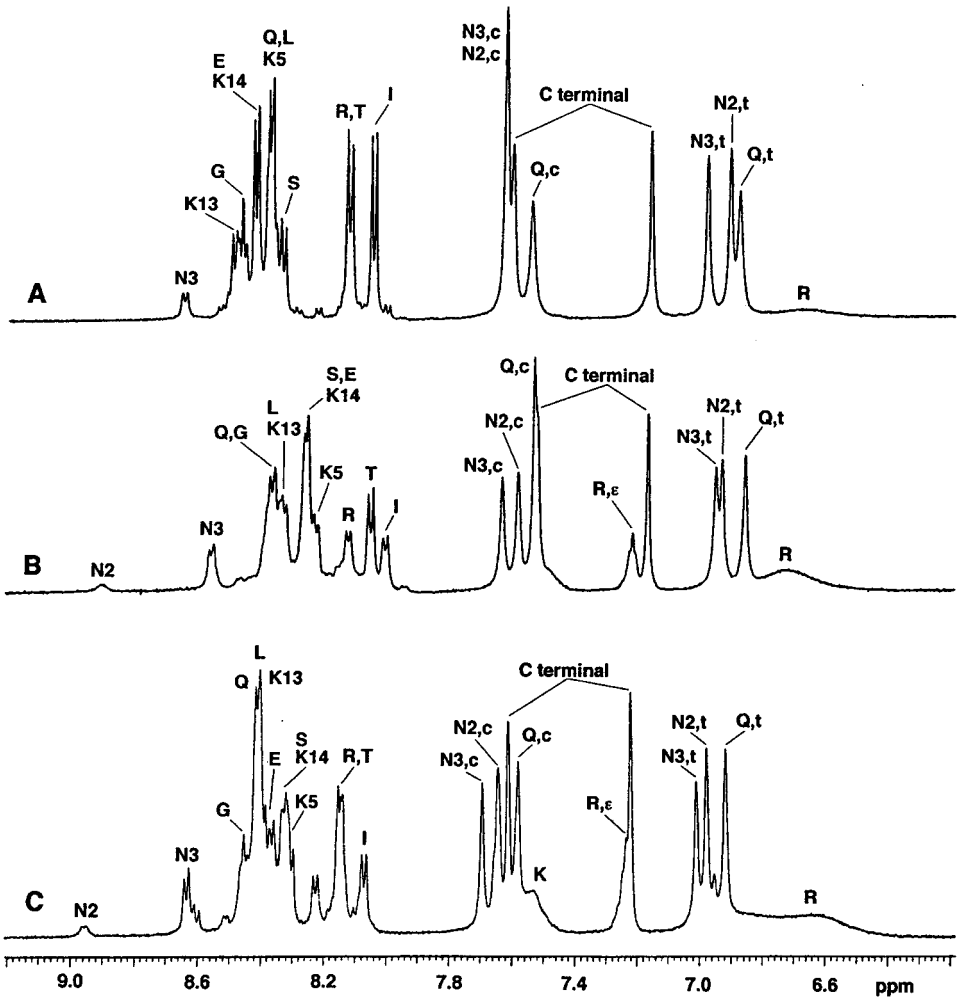

FIGURE 1: Amide region of 1D ^{1}H NMR spectra of (A) 5 mM FN-C/H II in 90% H_2O/10% D_2O at pH 5.5 and 25 °C, (B) 5 mM FN-C/H II plus 0.8 mM heparin in 90% H_2O/10% D_2O at pH 5.5 and 25 °C, and (C) 2.46 mM FN-C/H II plus 2.52 mM heparin hexasaccharide in 75% H_2O/25% D_2O at pH 5.35 and 15 °C. The broad resonance at ~7.52 ppm in spectrum C is from the lysine ammonium protons, the broad resonance at ~6.6 ppm is due to the arginine guanidinium protons. c and t refer to the *cis* and *trans* protons of side chain and C-terminal amide groups. The letters refer to the amino acids given in one letter code.

ppm) and the heparin anomeric protons (A1 and I1 of the A and I rings, 5−6 ppm) were used to access the individual amino acid spin systems of FN-C/H II and the monosaccharide spin systems of heparin, respectively, with two-dimensional NMR methods. Amide NH resonances were first assigned to amino acid spin systems using subspectra obtained from TOCSY spectra, and then sequence-specific assignments were made using through-space dipolar connectivities obtained from NOESY and ROESY spectra. Spectrum A in Figure 1 is the NH region of the 1D ^{1}H NMR spectrum of 5 mM FN-C/H II; spectrum B is for 5 mM FN-C/H II plus 0.8 mM heparin (~20 mM heparin disaccharide repeat unit). Both spectra were measured at pH 5.5 in 90% H_2O/10% D_2O. Resonances for the Asn and Gln side chain and the C-terminal amide protons (6.6−7.8 ppm) were assigned using NOESY cross-peaks. The unassigned low-intensity resonances in the 7.8−8.6 ppm region in Figure 1A are for peptide, which has the cis conformation across the Glu^7−Pro^8 peptide bond, as indicated by chemical exchange cross-peaks between these resonances and the more intense NH resonances for peptide, which has the trans conformation in ROESY spectra measured at 65 °C.

The chemical shifts of resonances for the peptide in solution with heparin are different, particularly those for the backbone amide NH and the $C_\alpha H$ protons. The NH resonances (Figure 1B) are broadened, and some which are absent from the spectrum of the free peptide are observed in the presence of heparin, including resonances for the backbone amide NH proton of Asn^2 and the $N_\epsilon H$ proton of Arg^{12}, and the intensity of the resonance for the backbone amide NH of Asn^3 is increased. Single resonances were observed for each peptide NH proton, rather than resonances for free and bound peptide, which indicates that either the peptide is essentially all in the bound form or, if a significant fraction is free, exchange between free and bound forms is fast on the NMR time scale. However, the line shapes and chemical shifts of the NH resonances are invariant at heparin disaccharide repeat unit:peptide ratios ≥4:1, which indicates that essentially all the peptide is bound.

Binding of peptides by heparin is primarily electrostatic in nature (*14*). FN-C/H II has six cationic groups which are potential sites of interaction with the anionic groups of heparin. If a specific ammonium group interacts with an anionic site on heparin, the interaction will cause an increase in its apparent pK_A (*56*). pK_A values were determined for the N-terminal ammonium group and for the ammonium group of each lysine side chain for both the free peptide and the peptide plus heparin using chemical shift−pD titration

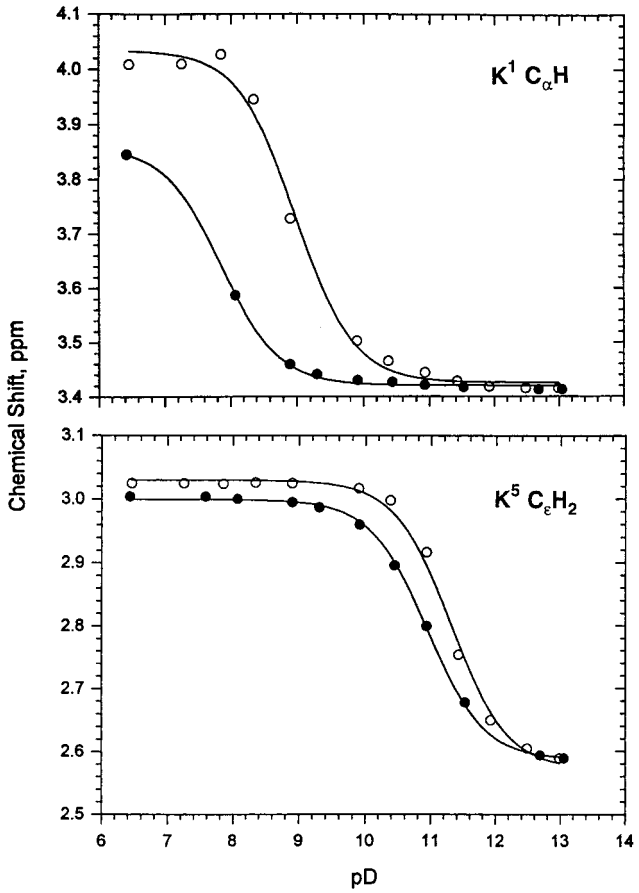

FIGURE 2: Chemical shift data for the $C_\alpha H$ proton of K^1 and the $C_\epsilon H_2$ protons of K^5 of FN-C/H II as a function of pD. The solid points are for free 10.2 mM FN-C/H II in D_2O, the open circles are for 10.5 mM FN-C/H II plus 1.6 mM heparin in D_2O, both at 25 °C. The curves through the points are predicted by the parameters obtained from the nonlinear least-squares fits to the data.

curves for the Lys^1 $C_\alpha H$ proton and the Lys^1, Lys^5, Lys^{13}, and Lys^{14} $C_\epsilon H_2$ protons. Chemical shift data were obtained for each lysine residue from 1D subspectra taken from two-dimensional TOCSY spectra. The subspectra were obtained by taking traces through the $C_\alpha H-C_\epsilon H_2$ cross-peaks, which are resolved for the four lysines because of small sequence-dependent differences in the chemical shifts of their $C_\alpha H$ protons (*57*).

Representative chemical shift−pD titration data obtained from TOCSY subspectra measured as a function of pD for free FN-C/H II and for FN-C/H II plus heparin are presented in Figure 2 for the resonances for the $C_\alpha H$ proton of Lys^1 and the $C_\epsilon H_2$ protons of Lys^5. Both chemical shift−pD titration curves are displaced to higher pD in the presence of heparin, indicating that the N-terminal and Lys^5 ammonium groups are involved in binding to heparin. Apparent pK_A values were determined for each of the five ammonium groups of free FN-C/H II and of FN-C/H II in solution with heparin by fitting the chemical shift−pD data by nonlinear least-squares methods to a monoprotic acid dissociation model (*57*). The results are reported in Table 1.

Chemical shift−pD data for the $C_\delta H_2$ protons of Arg^{12} of free FN-C/H II and of FN-C/H II plus heparin are plotted in Figure 3. At low pD, the chemical shift of the Arg^{12} $C_\delta H_2$ resonance is displaced downfield in the presence of heparin, which suggests that the guanidinium group of Arg^{12} is also

Table 1: Apparent Acid Dissociation Constants of the Ammonium Groups of FN-C/H II[a]

	FN-C/H II[b]	FN-C/H II + heparin[c]
N-terminal NH_3^+	7.86 ± 0.03	8.98 ± 0.06
K^1 side-chain NH_3^+	11.14 ± 0.01	11.29 ± 0.05
K^5 side-chain NH_3^+	10.95 ± 0.01	11.30 ± 0.05
K^{13} side-chain NH_3^+	10.96 ± 0.02	11.25 ± 0.06
K^{14} side-chain NH_3^+	11.09 ± 0.02	11.31 ± 0.06

[a] In D_2O at 25 °C. [b] 10.2 mM FN-C/H II. [c] 10.5 mM FN-C/H II, 1.6 mM heparin.

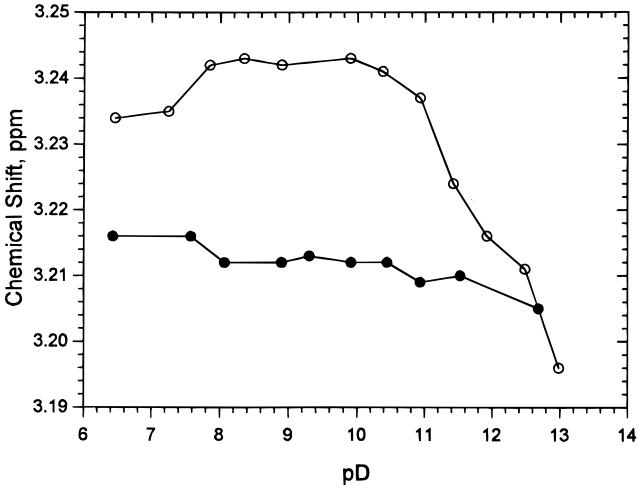

FIGURE 3: Chemical shift data for the $C_\delta H_2$ protons of R^{12} as a function of pD. The solid points are for free 10.2 mM FN-C/H II in D_2O, the open circles are for 10.5 mM FN-C/H II plus 1.6 mM heparin in D_2O, both at 25 °C.

involved in the binding of FN-C/H II by heparin. As the pD is increased from 10 to 12, the resonance shifts back to the chemical shift of free FN-C/H II. However, the pK_A of the guanidinium side chain is ~12.6, which suggests that this change in chemical shift is not due to titration of the guanidinium group. Rather, the chemical shift−pD titration behavior parallels that for the lysine $C_\epsilon H_2$ protons (Figure 2B), which suggests a decrease in the interaction of the guanidinium group with heparin when the lysine ammonium groups are titrated.

The chemical shifts of resonances for the carbon-bonded protons of heparin were also measured as a function of pD using one-dimensional subspectra obtained by taking traces through two-dimensional TOCSY spectra at the chemical shifts of the resolved A1, I1, and I5 resonances.[2] The chemical shifts of the various heparin resonances were the same over the pD range 6−12 for free heparin and for 0.8 mM heparin in solution with 5 mM FN-C/H II. To determine if the conformations across the glycosidic bonds of heparin change with peptide binding, NOESY spectra were measured for 0.4 mM heparin in D_2O at pD 7.4 and for 1.7 mM heparin plus 7.1 mM FN-C/H II in D_2O at pD 6.4. The intensity of the A1-I4 cross-peak decreased in the presence of peptide (data not shown), which suggests that the conformation across the [GlcNS(6S)]-(1→4)-[IdoA(2S)] glycosidic bond is slightly twisted compared to that of free heparin. However, the intensity of the I1−A4 NOE cross-peak is essentially

[2] Drake et al. report that weak NH-NH(i,i+1) NOEs were observed in a 600 MHz ^1H NOESY spectrum of the LIGRKKT segment of FN-C/H II at 5 °C and pH 6 (*41*).

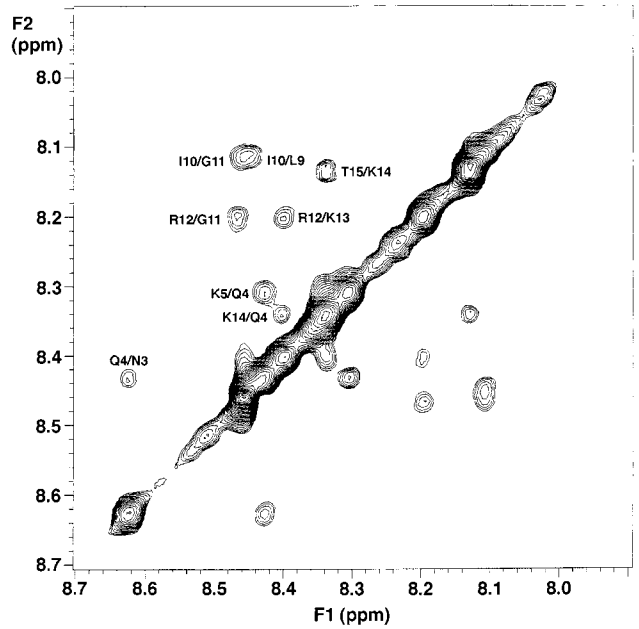

FIGURE 4: The NH-NH region of the NOESY spectrum of 5.1 mM FN-C/H II plus 1.5 mM heparin in 90% H_2O/10% D_2O at pH 5.5 and 15 °C. A total of 2432 data points were collected at 512 t_1 increments using a mixing time of 400 ms. The data were processed by zero filling to 4K and apodization with shifted sine-bell functions in both directions. The NH-NH(i,i+1) NOE cross-peaks are indicated, the NH-NH(i,i+2) cross-peaks listed in Table 2 are not visible at the vertical scale used to plot the spectrum.

the same for both free heparin and heparin plus peptide, which suggests no change in conformation across the [IdoA-(2S)]-(1→4)-[GlcNS(6S)] glycosidic bond.

Conformational Properties of FN-C/H II. ROESY and NOESY spectra were measured for FN-C/H II, free in solution and in solution with heparin. Conditions where NOESY cross-peaks are in the initial rate regime were established by measuring a series of NOESY spectra for pH 5.5 solutions containing 4 mM FN-C/H II and 4 mM FN-C/H II plus 0.8 mM heparin as a function of mixing time (50, 75, 100, 150, 200, and 400 ms). A mixing time of 200 ms was then used for conformational studies.

No backbone amide NH-NH NOEs were observed in either NOESY or ROESY spectra of free FN-C/H II.[2] However, in the presence of heparin, NH-NH(i,i+1) NOEs were observed in NOESY spectra for the sequences $N^3 - K^5$ and $L^9 - T^{15}$, as illustrated by the backbone amide NH-NH region of the NOESY spectrum of 5 mM FN-C/H II plus 1.6 mM heparin in Figure 4. The breaks in the sequential NH-NH NOEs are at proline and where NOEs, if present, could not be detected because the chemical shifts of the amide protons on adjacent residues are similar. The NH-NH NOEs in Figure 4 are summarized in Table 2, together with other NOEs which were observed in the presence of heparin. No intermolecular NOEs were observed between the protons of FN-C/H II and heparin.

Temperature coefficients for the chemical shifts of the backbone amide NH resonances (Table 3) are all smaller in the presence of heparin, which indicates increased protection of the amide protons from solvent (*58*). Protection of the amide protons from exchange with solvent protons is also indicated by 1D ^{1}H NMR spectra measured as a function of pH for FN-C/H II, free in solution and in the presence of heparin (Figure 5). The spectra show that essentially all the NH resonances are absent from the spectrum of the free peptide at pH 7.60 due to fast exchange with solvent protons, whereas most are observed at pH 7.65, and some are still detected at pH 8.7 (spectrum not shown) in the presence of heparin.

Competitive Binding of FN-C/H II and Na^+ by Heparin. Because of its high negative charge density, heparin is a polyelectrolyte, with a fraction of its negative charge neutralized by bound counterions (*59*−*69*). The ^{23}Na spin−lattice (T_1) relaxation time is less for Na^+ bound in the counterion condensation volume surrounding heparin than for free Na^+ (*59*, *69*, *70*). Displacement of bound Na^+ counterions by FN-C/H II (eq 1) was characterized using

$$\text{Peptide}^{n+}_{\text{(free)}} + m\text{Na}^+_{\text{(bound)}} \rightleftharpoons n\text{Na}^+_{\text{(free)}} + (m-n)\text{Na}^+_{\text{(bound)}} + \text{Peptide}^{n+}_{\text{(bound)}} \quad (1)$$

^{23}Na spin−lattice relaxation times.

Inversion−recovery data for solutions which contained NaCl, NaCl plus heparin, and NaCl plus heparin and FN-C/H II could all be fit by single-exponential functions, which indicates that exchange of Na^+ between its free and bound forms is fast on the NMR time scale (*70*). ^{23}Na spin−lattice relaxation rates ($=1/T_1$) are plotted as a function of pD in Figure 6 for solutions which contained (A) 68.8 mM NaCl, (B) 50.4 mM NaCl plus 0.11 mM heparin, and (C) 43.8 mM NaCl, 0.13 mM heparin, and 4.6 mM FN-C/H II. The total Na^+ concentration was the same within experimental error in each experiment. T_1 was also measured as a function of pD for 80 mM NaCl plus 2.5 mM FN-C/H II; the ^{23}Na T_1 was independent of pD and similar in magnitude to that observed for NaCl alone.

The relaxation rate for free Na^+ (curve A) is ∼21 s^{-1} ($T_1 \approx 48$ ms) and independent of pD. The relaxation rate for Na^+ in solution with heparin (curve B) is larger and is a function of pD due to both an increase in the number of bound Na^+ from 1.2 to 2.2/disaccharide repeat unit and a decrease in the T_1 of bound Na^+ from 11.5 to 3.7 ms upon titration of the carboxylic acid group (*59*). The relaxation rates observed for ^{23}Na in the heparin/FN-C/H II solution (curve C) lies between those for free Na^+ and for the sodium heparinate solution, which indicates displacement of bound Na^+ by FN-C/H II. The observed spin−lattice relaxation rate R_{1o} ($= 1/T_{1o}$) is the population weighted average of the relaxation rates of the free and bound forms of Na^+:

$$R_{1o} = p_f R_{1f} + p_b R_{1b} \quad (2)$$

where R_{1f} and R_{1b} and p_f and p_b are the relaxation rates and fractional populations of free and bound Na^+. Substitution of $1 = p_f + p_b$ into eq 2 gives the following equation for the fraction of bound Na^+:

$$p_b = (R_{1o} - R_{1f})/(R_{1b} - R_{1f}) \quad (3)$$

Using eq 3, the above values for T_{1f} and T_{1b}, the concentration of the heparin disaccharide repeat unit, and the total sodium concentration, we calculate from the observed relaxation rates in data set C in Figure 6 that FN-C/H II has displaced on average 1.0 Na^+ ion/heparin disaccharide repeat unit at pD 2.3, where heparin is in the CO_2H form and FN-C/H II has

Table 2: Summary of NOE Connectivities for FN-C/H II in Solution with Heparin[a]

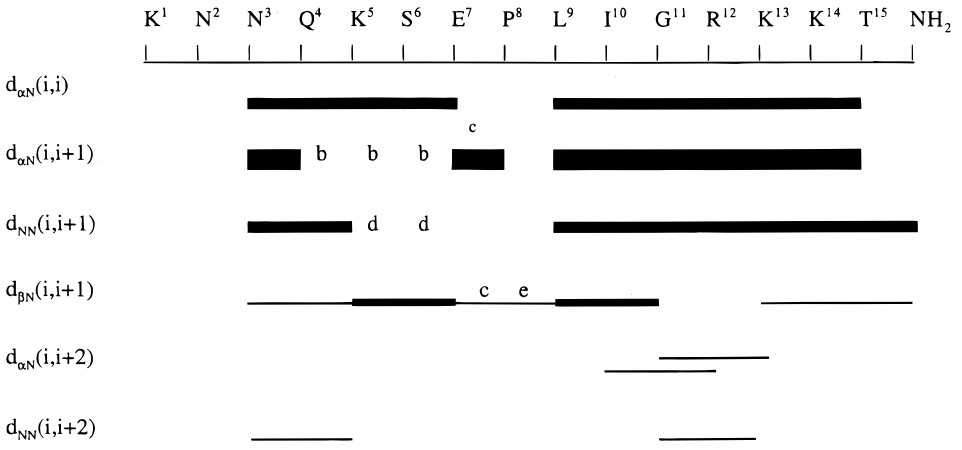

[a] 5 mM FN-C/H II, 0.8 mM heparin, 90% H_2O/10% D_2O, pH 5.50. The thicker the line, the stronger the NOE. [b] Unobservable if present due to overlap with other cross-peaks. [c] Pro $C_\delta H_2$. [d] Resonances of the NH protons on adjacent residues are nearly coincident. [e] Pro $C_\beta H_2$.

Table 3: Temperature Coefficients of the Chemical Shifts of the Amide Proton Resonances of FN-C/H II[a]

residue	FN-C/H II[b]	FN-C/H II + heparin[c]
Asn^3	6.35	5.67
Gln^4	6.16	5.72
Lys^5	6.98	5.17
Ser^6	6.68	5.66
Glu^7	6.80	5.79
Leu^9	7.45	6.50
Ile^{10}	7.75	6.70
Gly^{11}	6.60	5.34
Arg^{12}	6.18	5.22
Lys^{13}	7.46	5.70
Lys^{14}	6.50	5.39
Thr^{15}	6.21	5.71

[a] Values in negative units of ppb/K. [b] 5 mM FN-C/H II in 90% H_2O/10% D_2O at pH 5.5. The resonance for the Asn^2 NH proton was not observed at pH 5.5. [c] 5 mM FN-C/H II and 1.0 mM heparin in 90% H_2O/10% D_2O at pH 5.5.

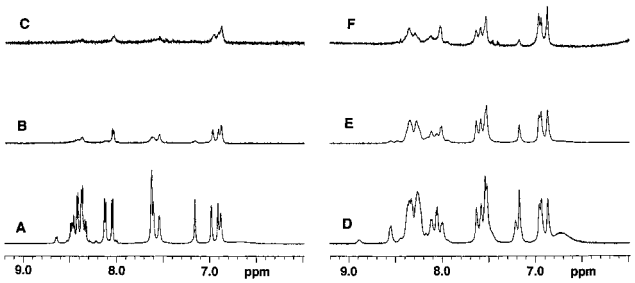

FIGURE 5: The NH region of 1D ^1H NMR spectra of 5 mM FN-C/H II at pH values of (A) 5.50, (B) 7.05, (C) 7.60 and of 5 mM FN-C/H II plus 0.8 mM heparin at pH values of (D) 5.44, (E) 6.99, and (F) 7.65. Both solutions were in 90% H_2O/10% D_2O. Spectra were measured at 25 °C with suppression of the H_2O resonance by presaturation.

a net charge of +6 and 2.0 Na^+ ions/disaccharide repeat unit at pD 5.9, where heparin is in the CO_2^- form and FN-C/H II has a net charge of +5. At pD greater than 7, where first the N-terminal ammonium group and then the lysine side-chain ammonium groups of FN-C/H II are titrated, the ^{23}Na relaxation rate increases, indicating a decrease in the number of Na^+ ions displaced by FN-C/H II to 0.9, 0.5, and 0.1 at pD 8.85, 10.27, and 11.28, respectively.

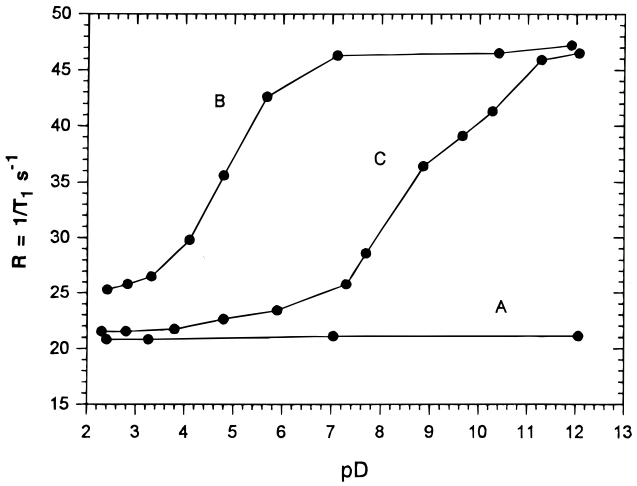

FIGURE 6: ^{23}Na relaxation rates as a function of pD for (A) 68.8 mM NaCl, (B) 0.11 mM heparin plus 50.4 mM NaCl (68 mM total Na^+), and (C) 4.6 mM FN-C/H II, 0.13 mM heparin and 43.8 mM NaCl (66 mM total Na^+) at 25 °C. The FN-C/H II plus heparin solution was slightly turbid over the pD range 4.8−7.7.

The competitive binding of FN-C/H II and Na^+ by heparin was also studied by heparin affinity chromatography. It was found that 0.313 M Na^+ was required to elute 1 mM FN-C/H II from the heparin affinity chromatography column at pH 5.5 (Table 4). The Na^+ concentration required to elute FN-C/H II from the heparin affinity column was also determined as a function of pH over the pH range 4.5−10. As the pH was increased over this pH range, the Na^+ concentration at which FN-C/H II was eluted decreased from 0.32 to 0.22 M, and the pH dependence of the required Na^+ concentration paralleled the titration of the N-terminal ammonium group (Figure 2).

Interaction of Analogue Peptides with Heparin. To determine the importance of individual basic residues on the interaction of FN-C/H II with heparin, the interaction of heparin with the series of analogue peptides in Table 4 was studied. The relative affinities of heparin for FN-C/H II and the analogue peptides were determined by heparin-affinity chromatography. The Na^+ concentrations at which the peptides were eluted from the heparin-affinity chromatography column are reported in Table 4.

Table 4: Heparin Affinity Chromatography Data for FN-CH II and for Analogues of FN-C/H II

peptide	substitution[a,b]	sequence	no. of cationic sites	NaCl concentration (M)[c]
FN-C/H II		KNNQKSEPLIGRKKT-NH_2	6	0.313
D-FN-C/H II		D-KNNQKSEPLIGRKKT-NH_2[d]	6	0.317
1	Ac, P8R	Ac-KNNQKSERLIGRKKT-NH_2	6	0.289
2	Ac, P8A	Ac-KNNQKSEALIGRKKT-NH_2	5	0.200
3	Ac-FN-C/H II	Ac-KNNQKSEPLIGRRKT-NH_2	5	0.188
4	Ac-D-FN-C/H II[d]	Ac-D-KNNQKSEPLIGRKKT-NH_2	5	0.191
5	Ac, K5A	AcKNNQASEPLIGRKKT-NH_2	4	0.144
6	Ac, K1A	Ac-ANNQKSEPLIGRKKT-NH2	4	0.141
7	Ac, K14A	Ac-KNNQKSEPLIGRKAT-NH_2	4	0.125
8	Ac, K13A	Ac-KNNQKSEPLIGRAKT-NH_2	4	0.122
9	Ac, R12A	Ac-KNNQKSEPLIGAKKT-NH_2	4	0.110
10	Ac, K1A, K5A	Ac-ANNQASEPLIGRKKT-NH_2	3	0.100
11	Ac, K13A, K14A	Ac-KNNQKSEPLIGRAAT-NH_2	3	0.053
12	Ac, R12A, K13A, K14A	Ac-KNNQKSEPLIGAAAT-NH_2	2	
13	Ac, K1A, K5A, P8A, K13A, K14A	Ac-ANNQASEALIGRAAT-NH_2	1	

[a] K1A indicates substitution of Lys^1 by Ala, etc. [b] Peptides 1−13 are all acetylated at the N-terminal amino group. [c] Calculated NaCl concentration at the peak maximum. [d] All D-amino acids.

Interaction of each of the analogue peptides with heparin was also studied by the same ^{1}H NMR methods used to characterize the interaction of FN-C/H II with heparin. The chemical shifts of analogue peptide resonances were different in the presence of heparin, particularly those for the backbone amide protons, indicating that all the analogue peptides interact with heparin, including analogues 12 and 13, which contain only one or two basic amino acid residues. However, the interaction of analogues 12 and 13 with heparin is weak, as indicated by the heparin affinity chromatography results. Two-dimensional NOESY spectra were measured for each peptide, both free in solution and in solution with heparin, using a 200 ms mixing time and a temperature of 15 °C. Strong sequential NH-NH(i,i+1) NOEs were observed for all the analogue peptides in the presence of heparin (data not shown). In some cases, NH-NH(i,i+1) NOEs were also observed for the peptides free in solution; however, the same NH-NH(i,i+1) cross-peaks in the presence of heparin were considerably more intense. For example, the NH(L^9)-NH(I^{10}), NH(I^{10})-NH(G^{11}), and NH(G^{11})-NH(R^{12}) NOEs for peptide 9 were 11, 8, and 6 times as large in the presence of heparin.

The interaction of heparin with the P8A analogue was studied to determine the effect of proline, a helix breaker, on the interaction of FN-C/H II with heparin. The helical-wheel representation of FN-C/H II shows that, in an α-helix, the side chains of its basic amino acids tend more or less to be on one side of the helix, which would maximize electrostatic interactions with the linear heparin polymer. However, the rather modest increase in the affinity of heparin for the P8A analogue as compared to analogue 3 in Table 4 suggests that, even after replacement of proline, there is little tendency for the bound peptide to have a helical secondary structure.

Interaction of D-FN-C/H II with Heparin. To determine if site-specific recognition plays a role in the interaction of FN-C/H II with heparin or if the interaction is mediated solely by nonspecific Coulombic forces between the positively charged side chains of FN-C/H II and the negatively charged groups on heparin, interaction of the D-amino acid analogues of FN-C/H II (D-FN-C/H II) and the N-terminal-acetyl derivative of FN-C/H II (Ac-D-FN-C/H II) with heparin was studied by heparin affinity chromatography and ^{1}H NMR. The NaCl concentrations at which FN-C/H II and D-FN-C/H II eluted from the heparin affinity chromatography column were identical, as were those for the D and L forms of the *N*-acetyl analogue (Table 4). Also, the ^{1}H NMR results for D-FN-C/H II in solution with heparin, including chemical shifts and NH-NH(i,i+1) NOEs, are the same as those obtained for FN-C/H II.

Binding of FN-C/H II by a Heparin-Derived Hexasaccharide. As discussed in the following section, the results from the ^{23}Na T_1 study of the displacement of Na^+ by FN-C/H II suggest that FN-C/H II binds to a hexasaccharide segment of heparin. To determine if a hexasaccharide is of sufficient length to bind heparin, the binding of FN-C/H II by the nonasulfated hexasaccharide Hexa1 was studied by ^{1}H NMR. Spectrum C in Figure 1 is the NH region of the 1D ^{1}H NMR spectrum of a solution of 2.46 mM FN-C/H II plus 2.52 mM Hexa1 in 75% H_2O/25% D_2O at 15 °C and pH 5.35. The pattern of resonances for the backbone amide protons is similar to that observed for FN-C/H II in solution with heparin (spectrum B in Figure 1), but with the resonances all shifted downfield due to the lower temperature. Also, as in spectrum B, the backbone amide NH resonance for Asn^2 and the $N_\epsilon H$ resonance for Arg^{12} are observed in spectrum C, and most of the sequential NH-NH cross-peaks and medium range cross-peaks observed for FN-C/H II in the presence of heparin (Table 2) were also observed in NOESY spectra for the FN-C/H II−hexasaccharide solution (data not shown).

DISCUSSION

Nature of the Interaction of FN-C/H II with Heparin. Heparin is a polyelectrolyte, with a fraction of its negative charge neutralized by bound counterions (*59*−*69*). According to Manning's counterion condensation theory of polyelectrolyte solutions, a polyelectrolyte is considered to be a uniform charged line of infinite length surrounded by a counterion condensation volume (*71*, *72*). Counterions in the condensation volume can interact with polyelectrolytes by delocalized, long-range electrostatic interactions and by direct binding to ionic sites. The ^{23}Na spin−lattice relaxation data

in Figure 6, together with the heparin affinity chromatography results for FN-C/H II and the analogue peptides in Table 4, provide direct evidence that Na^+ counterions are displaced when FN-C/H II interacts with heparin, i.e., the binding of FN-C/H II can be considered an ion exchange process with bound FN-C/H II serving as a counterion (eq 1).

The ^{23}Na relaxation data indicates displacement of 2.0 Na^+ ions/heparin disaccharide repeat unit by FN-C/H II at pH 5.9. Assuming a one-for-one replacement of Na^+ ions by cationic centers of FN-C/H II, this suggests that FN-C/H II binds to a hexasaccharide segment of heparin. This is consistent with the finding that there is no further change in the ^1H NMR spectrum of FN-C/H II at heparin disaccharide repeat unit-to-FN-C/H II ratios of $\geq$4:1, and it is consistent with the NMR results for FN-C/H II in solution with the hexasaccharide Hexa1, which indicate that Hexa1 interacts with FN-C/H II and induces the same secondary structure as the much larger heparin polymer.

Presumably, the five ammonium groups and the guanidinium group of FN-C/H II all contribute to its interaction with heparin via delocalized electrostatic interactions. They all are also involved in direct binding to anionic sites on heparin, as indicated by the increased pK_A values for the ammonium groups in the presence of heparin (Table 1), the chemical shifts of the resonances for the $C_\alpha H$ proton of Lys^1, the $C_\epsilon H_2$ protons of the four lysines, and the $C_\delta H_2$ protons of arginine of bound FN-C/H II, and observation of the resonance for the $N_\epsilon H$ proton of arginine in the presence of heparin. The crystal structure of a tosylarginine methyl ester/sulfonated azo dye complex indicates that the guanidinium group can interact directly with sulfonate groups by bridging the two terminal nitrogens, or the $N_\epsilon H$ nitrogen and a terminal nitrogen, via hydrogen bonding to two oxygens of the sulfonate group (*73*). Evidence has also been presented for interaction of the guanidinium group of the peptide *N*-acetyl-glycyl-argininyl-glycine-amide with the uronic acid carboxylate group of a heparin-derived disaccharide (*74*).

The Na^+ concentration required for elution of FN-C/H II and the analogue peptides from the heparin affinity chromatography column is dependent on peptide charge. However, there are small but significant differences in $[Na^+]_{elution}$ for analogue peptides of the same charge, which indicates that the basic amino acids do not all contribute equally to the affinity of heparin for FN-C/H II. The results for peptides 5−9 indicate that the relative contributions of the lysine and arginine residues to the affinity of heparin for FN-C/H II decreases in the order $R^{12} > K^{13} > K^{14} > K^1 > K^5$, which is consistent with the report that it is the carboxy-terminal LIGRKKT segment of FN-C/H II which mediates cell adhesion (*41*).

The observation of resonances for the exchangeable side-chain amide protons of Asn^2, Asn^3, and Gln^4 in spectrum F in Figure 5 indicates these protons are protected from exchange with solvent in the FN-C/H II−heparin complex, which suggests that the side-chain amide groups of the asparagine and glutamine residues are also sites of interaction with heparin. Precedent for the interaction of side-chain amide groups with heparin is provided by crystal structures of complexes of heparin-derived oligosaccharides with basic fibroblast growth factor, where the side chain amide groups of both asparagine and glutamine are involved in binding (*75*).

The ^1H NMR and heparin affinity chromatography results for the D-amino acid analogues of FN-C/H II and Ac−FN-C/H II provide additional information about the nature of the interaction of FN-C/H II with heparin. The chemical shift and NOE data for FN-C/H II and D-FN-C/H II in solution with heparin are identical, which indicates that heparin induces the same secondary structure in both FN-C/H II and its D-amino acid analogue. Also, the heparin affinity chromatography results indicate that the affinity of heparin for FN-C/H II and its D-amino acid analogue is the same. Taken together, these results provide evidence that the binding of FN-C/H II and its D-amino acid analogue by heparin is identical, which indicates that the binding interactions do not involve site-specific recognition of FN-C/H II by heparin, at least not by stretches of heparin comprised of the fully sulfated disaccharide repeat units which dominate the structure of bovine lung heparin.

Conformational Properties of FN-C/H II. Only NOEs typical of "random coil" peptides were observed in two-dimensional NOESY and ROESY spectra of FN-C/H II free in solution. Also, the temperature coefficients of the amide chemical shifts for the free peptide are all consistent with a largely unstructured peptide. NOE data clearly indicate, however, that heparin induces FN-C/H II into measurable populations of nonrandom conformations. The $d_{NN}(i,i+1)$, $d_{\alpha N}(i,i+2)$, and $d_{NN}(i,i+2)$ NOEs in Table 2 indicate at least a threshold population of conformers in which the distance between these protons is relatively short, and the extended sequence of $d_{\alpha N}(i,i+1)$ and $d_{NN}(i,i+1)$ NOEs is consistent with conformational averaging of the backbone dihedral angles of amino acids in the sequence between the α and β regions of ϕ,ψ space (*58*). Also, the temperature dependence of the chemical shifts of the backbone amide NH resonances, which in the presence of heparin (Table 3) is intermediate between that of free and hydrogen-bonded amide protons, indicates that heparin-bound FN-C/H II is in an equilibrium between conformations in which amide protons are protected from and exposed to solvent (*58*). However, interpretation of these results in terms of specific secondary structures is not straightforward because the bound peptide is interconverting among several conformational states and the NOEs reflect population weighted averages over those states. The sequential $d_{NN}(i,i+1)$ NOEs observed for the Leu^9-Thr^{15} segment, together with the $I^{10}-R^{12}$ and $G^{11}-K^{13}$ $d_{\alpha N}(i,i+2)$ NOEs, indicate that among these are turn-like conformations over the Leu^9-Thr^{15} segment.

CONCLUSIONS

The results of this study indicate that FN-C/H II binds to a hexasaccharide segment of heparin, that Na^+ ions are displaced upon the binding of FN-C/H II by heparin, and that the binding involves both delocalized and direct electrostatic interactions between cationic groups on FN-C/H II and anionic sites on heparin. The results also suggest that interactions between side chain amide groups and sites on heparin are involved in the binding, but that the binding does not involve site-specific recognition of FN-C/H II by heparin. However, the heparin used in this research was relatively homogeneous, with ~85% consisting of the repeating

trisulfated disaccharide [→4)-[IdoA(2S)]-(1→4)-[GlcNS-(6S)]-(1→], and thus the results do not rule out the possibility of site-specific recognition in the binding of FN-C/H II to unique, low-abundance oligosaccharide sequences in heparin. Since L-amino acid peptides are readily hydrolyzed by proteolytic enzymes, and thus are of limited use as therapeutic agents, the finding that the interaction of L- and D-amino acid forms of FN-C/H II with heparin is identical is of interest with respect to the potential use of peptides as therapeutic agents to interfere with the development of diseases in which cell adhesion plays a critical role.

SUPPORTING INFORMATION AVAILABLE

Tables listing complete ^{1}H NMR assignments for the free FN-C/H II in aqueous solution and in solution with heparin and the heparin-derived hexasaccharide. This material is available free of charge via the Internet at http://pubs.acs.org.

REFERENCES

1. Wahl, S. M., Allen, J. B., Hines, K. L., Imamichi, T., Wahl, A. M., Furcht, L. T., and McCarthy, J. B. (1994) *J. Clin. Invest. 94*, 655−662.
2. Wight, T. N., Kinsella, M. G., and Qwarnström, E. E. (1992) *Curr. Opin. Cell Biol. 4*, 793−801.
3. Liotta, L. A., Rao, C. N., and Wewer, U. M. (1986) *Annu. Rev. Biochem. 5*, 1037−1057.
4. McCarthy, J. B., Basara, M. L., Palm, S. L., Sas, D. F., and Furcht, L. T. (1985) *Cancer Metastasis Rev. 4*, 125−152.
5. Patel, H., Yanagishita, M., Roderiquez, G., Bou-Habib, D. C., Oravecz, T., Hascall, V. C., and Norcross, M. A. (1993) *AIDS Res. Hum. Retroviruses 9*, 167−174.
6. Shieh, M.-T., and Spear, P. G. J. (1994) *Virology 68*, 1224−1228.
7. Sawitzky, D., Voigt, A., and Habermehl, K.-O. (1993) *Med. Micorbiol. Immunol. 182*, 285−292.
8. Shieh, M.-T., WuDunn, D., Montgomery, R. I., Esko, J. D., and Spear, P. G. (1992) *J. Cell Biol. 116*, 1273−1281.
9. Pancake, S. J., Holt, G. D., Mellouk, S., and Hoffman, S. L. (1992) *J. Cell Biol. 117*, 1351−1357.
10. Ortega-Barria, E., and Pereira, M. E. A. (1991) *Cell 67*, 411−421.
11. Kjellen, L., and Lindahl, U. (1991) *Annu. Rev. Biochem. 60*, 443−475.
12. Yanagishita, M., and Hascall, V. C. (1992) *J. Biol. Chem. 267*, 9451−9454.
13. Bernfield, M., Kokenyesi, R., Kato, M., Hinkes, M. T., Spring, J., Gallo, R. L., and Lose, E. J. (1992) *Annu. Rev. Cell Biol. 8*, 365−393.
14. Lindahl, U., Lidholt, K., Spillman, D., and Kjellen, L. (1994) *Thromb. Res. 75*, 1−32.
15. Hynes, R. (1985) *Annu. Rev. Cell Biol. 1*, 67−90.
16. Skubitz, A. P. N., Letourneau, P. C., Wayner, E., and Furcht, L. T. (1991) *J. Cell. Biol. 115*, 1137−1148.
17. Burke, C., Mayo, K. H., Skubitz, A. P. N., and Furcht, L. T. (1991) *J. Cell Biol. 266*, 19407−19412.
18. Underwood, P. A., Dalton, B. A., Steele, J. G., Bennett, F. A., and Strike, P. (1992) *J. Cell Sci. 102*, 833−845.
19. Mooradian, D. L., McCarthy, J. B., Skubitz, A. P. N., Cameron, J. D., and Furcht, L. T. (1993) *Invest. Opthalmol. Vision Sci. 34*, 153−164.
20. Saiki, I., Iida, J., Murata, J., Ogawa, R., Nishi, N., Sugimura, K., Tokura, S., and Azuma, I. (1989) *Cancer Res. 49*, 3815−3822.
21. McCarthy, J. B., Chelberg, M. K., Mickelson, D. J., and Furcht, L. T. (1988) *Biochemistry 27*, 1380−1388.
22. Drake, S. L., Klein, D. J., Mickelson, D. J., Oegama, T. R., Furcht, L. T., and McCarthy, J. B. (1992) *J. Cell Biol. 117*, 1331−1341.
23. Guo, N.-H., Krutzsch, H. C., Negre, E.; Vogel, T., Blake, D. A., Roberts, D. D. (1992) *Proc. Natl. Acad. Sci. 89*, 3040−3044.
24. Barsky, S. H., Rao, C. N., Williams, J. E., and Liotta, L. A. (1984) *J. Clin. Invest. 74*, 843−848.
25. Humphries, M. J., Olden, L., and Yamada, K. M. (1986) *Science 233*, 467−470.
26. McCarthy, J. B., Skubitz, A. P. N., Palm, S. L., and Furcht, L. T. (1988) *J. Natl. Cancer Inst. 80*, 108−116.
27. Lindahl, U., and Höök, M. (1978) *Annu. Rev. Biochem. 47*, 385−417.
28. Jackson, R. L., Busch, S. J., and Cardin, A. D. (1991) *Physiol. Rev. 71*, 481−539.
29. Spillmann, D., and Lindahl, U. (1994) *Curr. Opin. Cell Biol. 4*, 677−682.
30. Cardin, A. D., and Weintraub, H. J. R. (1989) *Arteriosclerosis 9*, 21−32.
31. Cardin, A. D., Demeter, D. A., Weintraub, H. J. R., and Jackson, R. L. (1991) *Methods Enzymol 203*, 556−583.
32. Gallagher, J. T., Lyon, M., and Steward, W. P. (1986) *Biochem. J. 236*, 313−325.
33. Lindahl, U., Feingold, D. S., and Roden, L. (1986) *Elsevier Science Publishers 86*, 221−225.
34. Casu, B. (1985) *Adv. Carbohydr. Chem. Biochem. 43*, 51−134.
35. Gallagher, J. T. (1987) *Nature 326*, 136.
36. Lortat-Jacob, H., and Grimaud, J.-A. (1992) *Biochim. Biophys. Acta 1117*, 126−130.
37. Nader, H. B., Dietrich, C. P., Buonassisi, V., and Colburn, P. (1987) *Proc. Natl. Acad Sci. U.S.A. 84*, 3565−3569.
38. Lane, D. A. (1989) in *Heparin: Chemical and Biological Properties, Clinical Applications* (Lane, D. A., and Lindahl, U., Eds.) pp 363−391, CRC Press, Boca Raton.
39. Haugen, P. K., McCarthy, J. B., Skubitz, A. P. N., Furcht, L. T., and Letourneau, P. C. (1990) *J. Cell Biol. 111*, 2733−2745.
40. Haugen, P. K., Letourneau, P. C., Drake, S. L., Furcht, L. T., and McCarthy, J. B. (1992) *J. Neurosci. 12*, 2597−2608.
41. Drake, S. L., Varnum, J., Mayo, K. H., Letourneau, P. C., Furcht, L. T., and McCarthy, J. B. (1993) *J. Biol. Chem. 268*, 15859−15867.
42. King, D. S., Fields, C. G., and Fields, G. B. (1990) *Int. J. Pept. Res. 36*, 255−266.
43. Bax, A., and Davis, D. G. (1985) *J. Magn. Reson. 65*, 355−360.
44. Davis, D. G., and Bax, A. (1985) *J. Am. Chem. Soc. 107*, 2820−2821.
45. Jeener, J., Meier, B. H., Bachman, P., and Ernst, R. R. (1979) *J. Chem. Phys. 71*, 4546−4563.
46. Bothner-By, A. A., Stephens, R. L., Lee, J.-M., Warren, C. D., and Jeanloz, R. W. (1984) *J. Am. Chem. Soc. 106*, 811−813.
47. Bax, A., and Davis, D. G. (1985) *J. Magn. Reson. 63*, 207−213.
48. States, D. J., Habercorn, R. A., and Ruben, D. J. (1982) *J. Magn. Reson. 48*, 286−292.
49. Glasoe, P. K., and Long, F. A. (1960) *J. Phys. Chem. 64*, 188−190.
50. Rice, K. G., and Linhardt, R. J. (1989) *Carbohydr. Res. 190*, 219−233.
51. Horne, A., and Gettins, P. (1991) *Carbohydr Res. 225*, 43−57.
52. Larnkjaer, A., Hansen, S. H., and Ostergaard, P. B. (1995) *Carbohydr. Res. 266*, 37−52.
53. Pervin, A., Gallo, C., Jandik, K. A., Han, X.-J., and Linhardt, R. J. (1995) *Glycobiology 5*, 83−95.
54. Redfield, C. (1993) in *NMR of Macromolecules: A Practical Approach* (Roberts, G. C. K., Ed.) pp 71−99, Oxford University Press, Oxford.
55. Homans, S. W. (1993) in *NMR of Macromolecules: A Practical Approach* (Roberts, G. C. K., Ed.) pp 289−313, Oxford University Press, Oxford.
56. Rabenstein, D. L., Bratt, P., Schierling, T. D., Robert, J. M., and Guo, W. (1992) *J. Am. Chem. Soc. 114*, 3278−3285.

57. Rabenstein, D. L., Hari, S. P., and Kaerner, A. (1997) *Anal. Chem. 69*, 4310−4316.
58. Dyson, H. J., and Wright, P. E. (1991) *Annu. Rev. Biophys. Biophys. Chem. 20*, 519−538.
59. Rabenstein, D. L., Robert, J. M., and Peng, J. (1995) *Carbohydr. Res. 278*, 239−256.
60. Casu, B. (1985) *Adv. Carbohydr. Chem. 43*, 51−134.
61. Mattai, J., and Kwak, J. C. T. (1981) *Biochim. Biophys. Acta 677*, 303−310.
62. Mattai, J., and Kwak, J. C. T. (1988) *Biophys. Chem. 31*, 295−299.
63. Dais, P., Peng, Q.-J., and Perlin, A. S. (1987) *Can. J. Chem. 65*, 1739−1745.
64. Dais, P., Peng, Q.-J., and Perlin, A. S. (1987) *Carbohydr. Res. 168*, 163−179.
65. Ascoli, F., Botre, C., and Liquori, A. M. (1961) *J. Phys. Chem. 65*, 1991−1992.
66. Diakun, G. P., Edwards, H. E., Wedlock, D. J., Allen, J. C., and Phillips, G. O. (1978) *Macromolecules 11*, 1110−1114.
67. Villiers, C., Brand, C., and Vert, M. (1980) *Carbohydr. Res. 83*, 335.
68. Brand, C., Villiers, C., and Vert, M. (1980) *Carbohydr. Res. 86*, 165−175.
69. Delville, A., and Laszlo, P. (1983) *Biophys. Chem. 17*, 119−124.
70. Lerner, L., and Torchia, D. A. (1986) *J. Biol. Chem. 261*, 12706−12714.
71. Manning, G. S. (1979) *Acc. Chem. Res. 12*, 443−449.
72. Manning, G. S. (1978) *Q. Rev. Biophys. 11*, 179−246
73. Ojala, W. H., Sudbeck, E. A., Lu, L. K., Richardson, T. I., Lovrien, R. E., and Gleason, W. G. (1996) *J. Am. Chem. Soc. 118*, 2131−2142.
74. Mikhailov, D., Mayo, K. H., Pervin, A., and Linhardt, R. J. (1996) *Biochem. J. 315*, 447−454.
75. Faham, S., Hileman, R. E., Fromm, J. R., Linhardt, R. J., and Rees, D. C. (1996) *Science 271*, 1116−1120.

BI9926734